Available online at www.sciencedirect.com

SciVerse ScienceDirect

Ceramics International 38 (2012) 2951–2956

CERAMICS INTERNATIONAL

www.elsevier.com/locate/ceramint

Synthesis and negative thermal expansion properties of solid solutions $Yb_{2-x}La_xW_3O_{12}$ ($0 \leq x \leq 2$)

Hongfei Liu [a,*], Wei Zhang [a], Zhiping Zhang [b], Xiaobing Chen [a]

[a] School of Physics Science and Technology, Yang Zhou University, Yang Zhou 225009, PR China

[b] Department of Electrical and Mechanical Engineering, Jianghai College, Yang Zhou 225009, PR China

Received 3 November 2011; received in revised form 25 November 2011; accepted 26 November 2011

Available online 4 December 2011

Abstract

A new series of rare earth solid solutions $Yb_{2-x}La_xW_3O_{12}$ were successfully synthesized by the solid-state method. Effects of substituted ion lanthanum on the microstructures and thermal expansion properties in the resulting $Yb_{2-x}La_xW_3O_{12}$ ceramics were investigated by X-ray diffraction (XRD), thermogravimetric analyzer (TGA), field emission scanning electron microscope (FESEM) and thermal mechanical analyzer (TMA). Results indicate that the structural phase transition of the $Yb_{2-x}La_xW_3O_{12}$ changes from orthorhombic to monoclinic with increasing substituted content of lanthanum. The pure phases can form in the composition range of $0 \leq x < 0.5$ with orthorhombic structure and $1.5 < x \leq 2$ with monoclinic one. High lanthanum content leads to a low hygroscopicity of $Yb_{2-x}La_xW_3O_{12}$. Negative thermal coefficients of the $Yb_{2-x}La_xW_3O_{12}$ ($0 \leq x \leq 2$) also vary from $-7.78 \times 10^{-6}\,K^{-1}$ to $2.06 \times 10^{-6}\,K^{-1}$ with increasing substituted content of lanthanum.

Keywords: C. Thermal expansion; Solid solution; Tungstates

1. Introduction

Thermal expansion is one of the properties which must be considered in the application of highly functional materials because the mismatch of thermal expansion between component materials can cause problems, such as mechanical destruction and positional deviation, in electrical, optical and high-temperature devices. One of the possible methods that can solve these problems is preparing materials with controllable or near-zero expansion coefficients. A simple idea to prepare them is combining negative thermal expansion (NTE) materials with positive thermal expansion materials [1–6].

Recently, the family $A_2W_3O_{12}$ materials have attracted widespread interest due to their larruping thermal expansion properties. The thermal expansion coefficients of $A_2W_3O_{12}$ can be tailored to be positive or negative by changing the A cation. Some compounds of the type $A_2W_3O_{12}$ materials have been reported. It has been found that there are two structures in the family $A_2W_3O_{12}$ compounds, orthorhombic and monoclinic, and thermal expansion properties are mainly related to the structures. Compounds with orthorhombic structure exhibit negative thermal expansion, such as $Sc_2W_3O_{12}$ [7,8], $Y_2W_3O_{12}$ [9,10], $Er_2W_3O_{12}$ [10,11] and $Lu_2W_3O_{12}$ [12], this orthorhombic structure is composed of corner-shared AO_6 octahedra and WO_4 tetrahedra. A–O–W linkages in their structure can accommodate transverse thermal vibrations and lead to the NTE [13]. Compounds with monoclinic structure exhibit positive thermal expansion, such as $La_2W_3O_{12}$ [10], $Dy_2W_3O_{12}$ [10], and $Nd_2W_3O_{12}$ [10], this monoclinic structure is composed of edge-sharing AO_8 polyhedra and WO_4 tetrahedra.

It is reported that controllable thermal expansion coefficient in $A_2W_3O_{12}$ may be obtained by partial chemical substitution of the "A" cation by another trivalent cation [1,14–17]. $Yb_2W_3O_{12}$ crystallizes in an orthorhombic symmetry (*Pnca*) and exhibits NTE with the linear thermal expansion coefficient of $-9.65 \times 10^{-6}\,K^{-1}$ in the temperature range from 373 K to 873 K [10,11]. Whereas, $La_2W_3O_{12}$ crystallizes in a monoclinic symmetry (*C2/c*) and exhibits positive thermal expansion with the linear thermal expansion coefficient of $4.14 \times 10^{-6}\,K^{-1}$ in the temperature range from room temperature to 1073 K [10]. It is therefore possible to obtain the solid solutions $Yb_{2-x}La_xW_3O_{12}$ with controllable thermal expansion coefficient by

* Corresponding author. Tel.: +86 514 87979022; fax: +86 514 87979244.
E-mail address: liuhf@yzu.edu.cn (H. Liu).

0272-8842/$36.00
doi:10.1016/j.ceramint.2011.11.072

partial substitution of Yb^{3+} with La^{3+}, and control the thermal expansion coefficient to be negative, positive and even zero by careful adjustment of the Yb/La ration.

In this paper, a series of $Yb_{2-x}La_xW_3O_{12}$ $(0 \leq x \leq 2)$ ceramics were successfully prepared by solid-state reaction and the effects of substituted lanthanum content on the microstructure and thermal expansion were also studied.

2. Experimental

2.1. Preparation of the $Yb_{2-x}La_xW_3O_{12}$ $(0 \leq x \leq 2)$ samples

All the $Yb_{2-x}La_xW_3O_{12}$ $(0 \leq x \leq 2)$ solid solutions were synthesized by the conventional solid-state reaction method from the corresponding oxides Yb_2O_3 (purity ≥99.9%), La_2O_3 (purity ≥99.5%) and WO_3 (purity ≥99.5%). All the starting materials were preheated at 300 °C for 24 h before weighting to protect from H_2O. Stoichiometric ratios of the reactants were fully ground together and then pressed into pellets. The pellets were calcined at 1000 °C in air for 24 h with an intermediate regrinding.

2.2. Experimental techniques

The resulting samples were characterized by powder X-ray diffraction (XRD) using Cu Ka radiation ($\lambda = 0.15418$ nm) with 40 kV/200 mA (D/max2500, Rigaku). The XRD data were collected with a scanning speed of 5° (2θ)/min in the 2θ range from 10° to 40° by continuum scanning method. The thermogravimetric curves of the samples were collected in the open air from room temperature to 300 °C using thermogravimetric analyzer (TGA, Pyris1). The heating rate is 10 °C/min. The microstructures of the samples were observed by a field emission scanning electron microscope (FESEM, Hitachi S-4800) under an acceleration voltage of 15 kV. Densities of the samples were measured using Archimedes' method. The thermal expansion coefficients of the samples were measured by thermal mechanical analyzer (TMA/SS, Seiko 6300). The measurements were carried out at the rate of 10 °C/min in the open air from room temperature to 700 °C.

3. Results and discussion

3.1. XRD analysis

Phase identifications of compounds $Yb_{2-x}La_xW_3O_{12}$ were carried out by X-ray powder diffraction. Fig. 1 shows the typical XRD patterns of the obtained $Yb_{2-x}La_xW_3O_{12}$ ($x = 0$, 0.25, 0.5, 1, 1.5, 1.75, 2) ceramics. Owing to the difference between $Yb_2W_3O_{12}$ (monoclinic, *C*2/*c*) and $La_2W_3O_{12}$ (orthorhombic, *Pnca*) in their structures and their cation radius, solid solutions $Yb_{2-x}La_xW_3O_{12}$ only can form in certain composition range by solid state reaction. As one can see in Fig. 1, the $Yb_{2-x}La_xW_3O_{12}$ ($x = 1.5$, 1.75, 2) synthesized with different amount of lanthanum have almost the same XRD patterns, and all the peak positions of

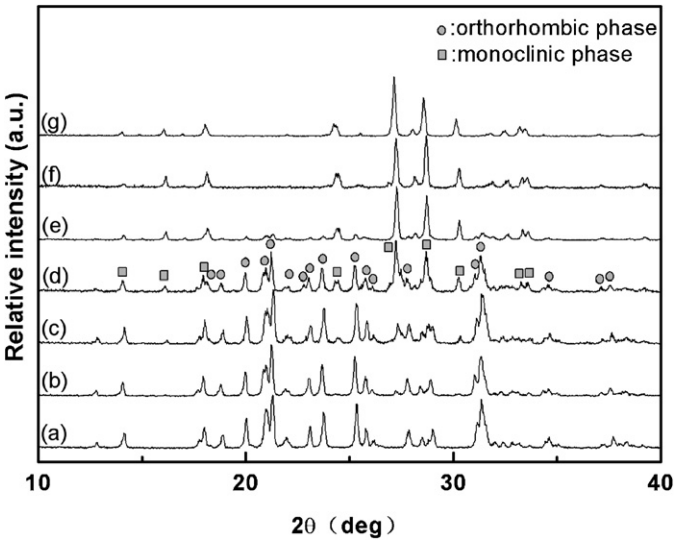

Fig. 1. XRD patterns of the obtained $Yb_{2-x}La_xW_3O_{12}$ ($x = 0$, 0.25, 0.5, 1, 1.5, 1.75, 2) ceramics (a) $Yb_2W_3O_{12}$; (b) $Yb_{1.75}La_{0.25}W_3O_{12}$; (c) $Yb_{1.5}La_{0.5}W_3O_{12}$; (d) $Yb_1La_1W_3O_{12}$; (e) $Yb_{0.5}La_{1.5}W_3O_{12}$; (f) $Yb_{0.25}La_{1.75}W_3O_{12}$; (g)$La_2W_3O_{12}$.

these samples are well indexed to the $La_2W_3O_{12}$ (JCPDS 15-0438) except $Yb_{0.5}La_{1.5}W_3O_{12}$, several little peaks ascribed to $Yb_2W_3O_{12}$ can be seen in Fig. 1(e), indicating pure phase of $Yb_{2-x}La_xW_3O_{12}$ can form in the composition range of $1.5 < x \leq 2$ with monoclinic structure. Comparing with the XRD patterns of the $Yb_{2-x}La_xW_3O_{12}$ ($x = 1.5$, 1.75, 2), it is found that all the diffraction angels shift towards higher 2θ angles with the increase of the amount of ytterbium ions, which can be obviously seen in Fig. 2. The refined cell parameters and volumes of $Yb_{2-x}La_xW_3O_{12}$ ($x = 1.6$, 1.7, 1.8, 1.9, 2) were also measured by XRD and then calculated by Powder X software. As shown in Fig. 3, it can be seen that the lattice parameters *a*–*c* and *V* increase gradually with the increasing lanthanum content owing to the ionic radii of La^{3+} (106.1 pm) is larger than that of Yb^{3+} (85.8 pm). This is in good agreement with the Vegard's law, and

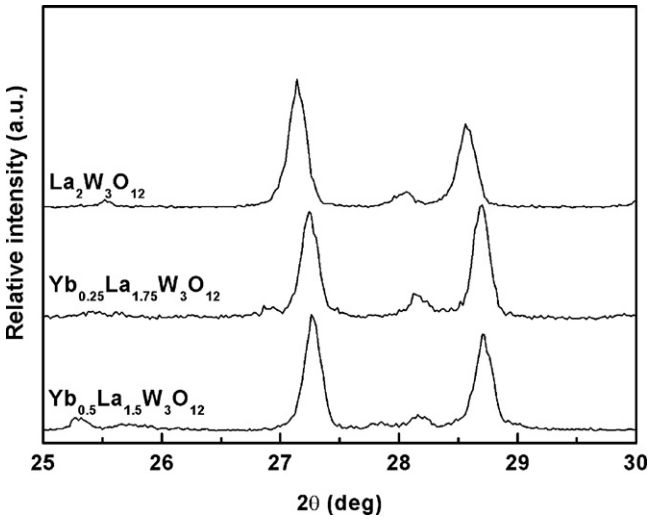

Fig. 2. Part XRD patterns of the obtained $Yb_{2-x}La_xW_3O_{12}$ ($x = 1.5$, 1.75, 2) ceramics.

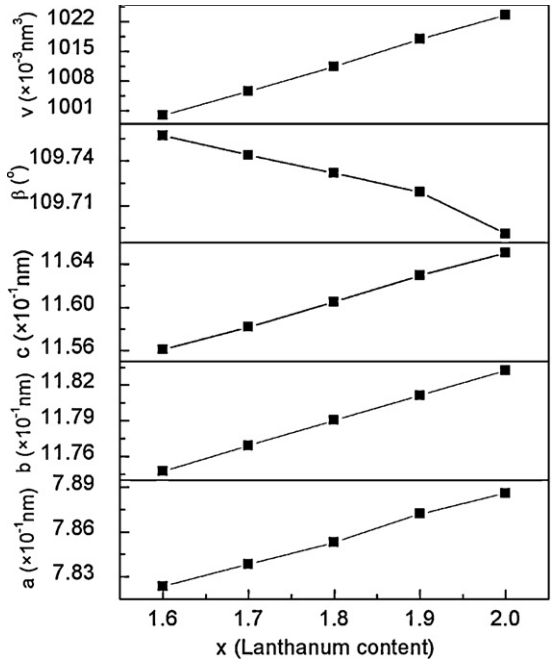

Fig. 3. The lattice parameters of solid solutions $Yb_{2-x}La_xW_3O_{12}$ (x = 1.6, 1.7, 1.8, 1.9, 2) at room temperature as a function of lanthanum content.

on the other hand it also proves that the $Yb_{2-x}La_xW_3O_{12}$ ($1.5 < x \leq 2$) compounds have been successfully synthesized.

As shown in Fig. 1 the samples $Yb_{2-x}La_xW_3O_{12}$ ($0.5 \leq x \leq 1.5$) are biphasic mixtures, they contain both monoclinic and orthorhombic phases, and some representative reflections of the two phases are labeled in Fig. 1(d). The $Yb_{2-x}La_xW_3O_{12}$ also can form pure phase in the composition range of $0 \leq x < 0.5$ with orthorhombic structure. The XRD patterns of the $Yb_{2-x}La_xW_3O_{12}$ (x = 0, 0.25, 0.5, 1) are similar to that reported for $Yb_2W_3O_{12}{\cdot}nH_2O$, which is hygroscopic at room temperature [10]. The board humps in the XRD patterns indicate that some amorphous phase might form owing to the absorption of water molecules in the frame-structure.

3.2. Thermogravimetric analysis

Thermogravimetric (TG) curves of the obtained $Yb_{2-x}La_xW_3O_{12}$ (x = 0, 0.25, 0.5, 1, 1.5, 1.75, 2) samples are shown in Fig. 4. It can be found that samples $Yb_{2-x}La_xW_3O_{12}$ (x = 0.25, 0.5, 1, 1.5, 1.75, 2) are hygroscopic at room temperature and the water molecules escape in the temperature range from 40 °C to 80 °C, and the mass loss are about 4.53%, 4.01%, 3.59%, 2.44%, 1.00% and 0.32%, respectively. The corresponding numbers of water molecules per formula unit are calculated to be 2.87, 2.53, 2.25, 1.51, 0.61 and 0.19. This hygroscopic phenomenon also has been found in some other orthorhombic $A_2W_3O_{12}$ (A = Er, Lu and Y) [10–12]. However, there is no obvious inclination can be observed from 40 °C to 80 °C in the TG curves of the $La_2W_3O_{12}$, indicating no water of adsorbed moisture in the samples. Based on the above TG analysis, it can be obviously found that the hygroscopic phenomenon of the $Yb_{2-x}La_xW_3O_{12}$ (x = 0, 0.25, 0.5, 1, 1.5, 1.75, 2) samples are improved with more Yb^{3+} replaced by La^{3+}.

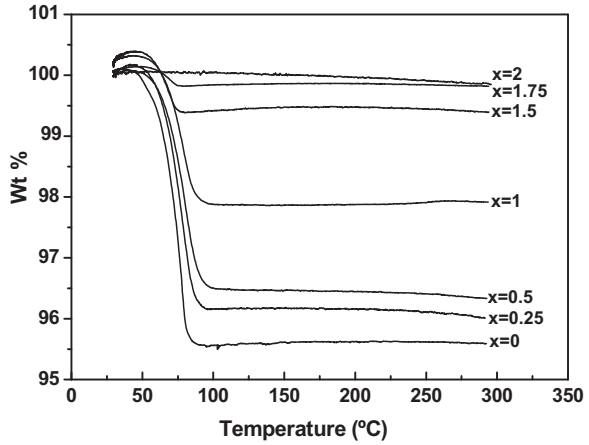

Fig. 4. Thermogravimetric curves of the obtained $Yb_{2-x}La_xW_3O_{12}$ samples (x = 0, 0.25, 0.5, 1, 1.5, 1.75, 2).

3.3. SEM images and density analysis

The SEM fractographs of the obtained $Yb_{2-x}La_xW_3O_{12}$ (x = 0, 0.25, 0.5, 1, 1.5, 1.75, 2) ceramics are shown in Fig. 5. More interestingly, The SEM fractographs of the $Yb_{2-x}La_xW_3O_{12}$ (x = 0.25, 0.5, 1, 1.5, 1.75) ceramics are different with the $Yb_2W_3O_{12}$ and $La_2W_3O_{12}$. In Fig. 4(a) and (g), it can be seen that the microstructures of the $Yb_2W_3O_{12}$ and $La_2W_3O_{12}$ ceramic are almost same, and they both consisted of small grains and with lots of pores inside. However, the grain sizes of the $Yb_2W_3O_{12}$ are larger than those of $La_2W_3O_{12}$. Comparing with the $La_2W_3O_{12}$ and $Yb_2W_3O_{12}$ ceramics, the $Yb_{2-x}La_xW_3O_{12}$ (x = 0.25, 0.5, 1, 1.5, 1.75) ceramics contained larger grains, meanwhile, the pores almost disappeared and the samples became denser. However, there are still some microcracks existed in $Yb_{2-x}La_xW_3O_{12}$ (x = 0.25, 0.5, 1, 1.5, 1.75) ceramics due to the large grain size and anisotropy in grain shape. According to the SEM results, it can be concluded that the microstructures and densities of the $Yb_{2-x}La_xW_3O_{12}$ ($0 \leq x \leq 2$) are affected by the substituted lanthanum and obviously improved. Further work is in the progress to investigate the formation mechanism in detail.

To further investigate the densities of the resulting $Yb_{2-x}La_xW_3O_{12}$ (x = 0, 0.25, 0.5, 1, 1.5, 1.75, 2) ceramics, the densities of the samples were measured using Archimedes' method [15] and the theoretical densities were calculated from theoretical values for $La_2W_3O_{12}$ (6.63 g/cm^3) and $Yb_2W_3O_{12}$ (6.79 g/cm^3). The testing results are in good accordance with the SEM analysis, as shown in Table 1, the testing density of $La_2W_3O_{12}$ and $Yb_2W_3O_{12}$ are 5.43 g/cm^3 and 5.66 g/cm^3, which reaches 81.91% and 83.33% of the theoretical density values, respectively. Compared with $La_2W_3O_{12}$ and $Yb_2W_3O_{12}$, the relative densities of the $Yb_{2-x}La_xW_3O_{12}$ (x = 0.25, 0.5, 1, 1.5, 1.75) ceramics can reach 93.63%, 91.84%, 94.37%, 90.89% and 92.71% of the theoretical values, respectively. The densities of $Yb_{2-x}La_xW_3O_{12}$ (x = 0.25, 0.5, 1, 1.5, 1.75) ceramics significantly improved and became denser.

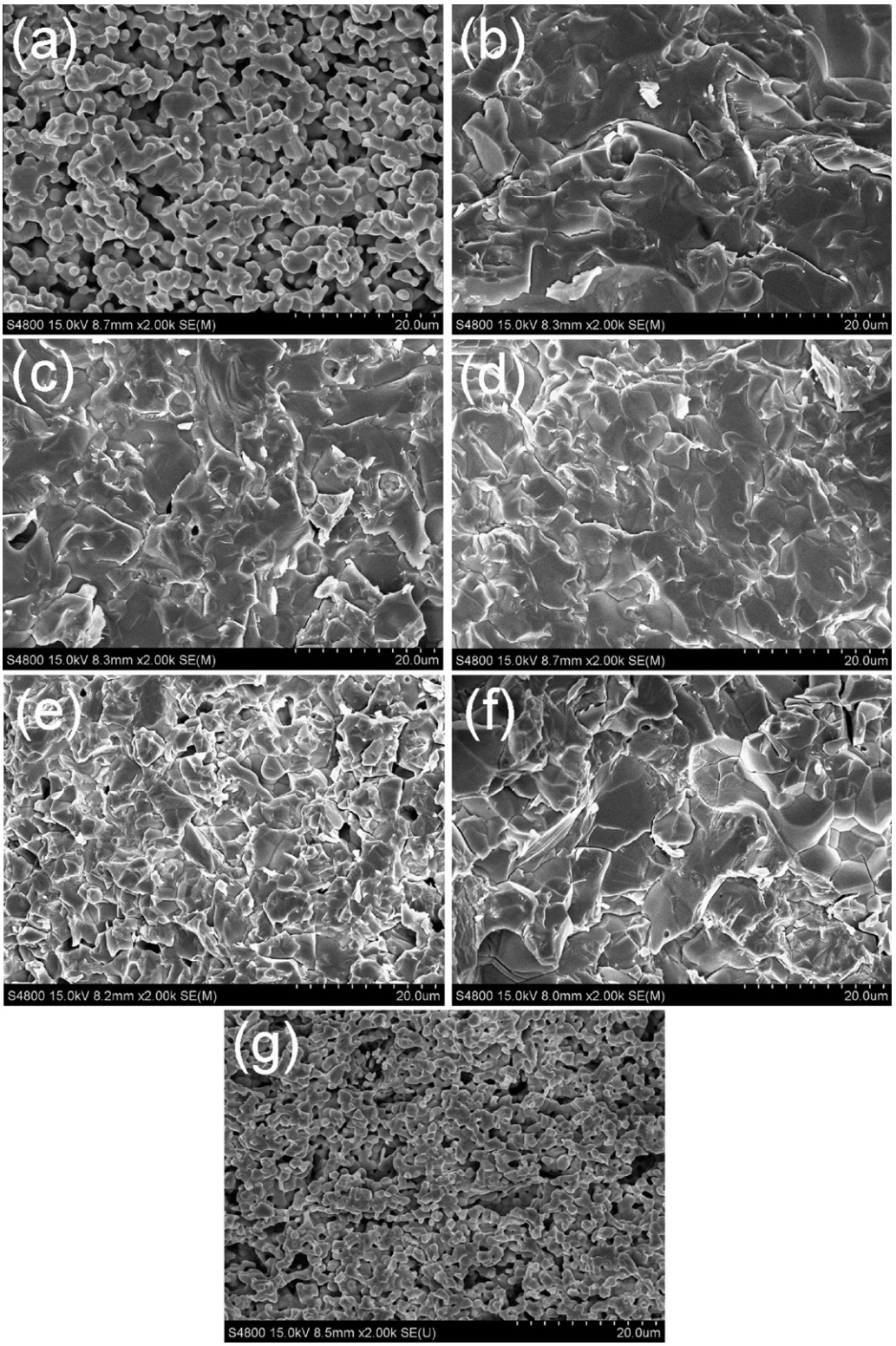

Fig. 5. SEM images of the obtained $Yb_{2-x}La_xW_3O_{12}$ ($x = 0$, 0.25, 0.5, 1, 1.5, 1.75, 2) ceramics (a) $Yb_2W_3O_{12}$; (b) $Yb_{1.75}La_{0.5}W_3O_{12}$; (c) $Y_{1.5}La_{0.5}W_3O_{12}$; (d) $Yb_1La_1W_3O_{12}$; (e) $Yb_{0.5}La1_{1.25}W_3O_{12}$; (f) $Yb_{0.25}La_{1.75}W_3O_{12}$; (g) $La_2W_3O_{12}$.

3.4. Thermal expansion properties

The thermal expansion curves of the obtained $Yb_{2-x}La_xW_3O_{12}$ ($x = 0$, 0.25, 0.5, 1, 1.5, 1.75, 2) ceramics are shown in Fig. 6. It can be seen that the thermal expansion curves of the $Yb_{2-x}La_xW_3O_{12}$ ($x = 0$, 0.5, 1, 1.5, 1.75) ceramics all show an initial expansion due to the removal of the water molecules, which is also supported from the above thermogravimetric analysis. The general features of these materials in the thermal expansion behaviors are similar to the thermal expansion of the

Table 1
Theoretical densities and testing densities of $Yb_{2-x}La_xW_3O_{12}$ ($x = 0$, 0.25, 0.5, 1, 1.5, 1.75, 2) ceramics.

$Yb_{2-x}La_xW_3O_{12}$	Theoretical density (g/cm^3)	Testing density (g/cm^3)	Testing density/theoretical density
$x = 0$	6.79	5.66	83.33%
$x = 0.25$	6.78	6.35	93.63%
$x = 0.5$	6.75	6.20	91.84%
$x = 1$	6.71	6.33	94.37%
$x = 1.5$	6.67	6.06	90.89%
$x = 1.75$	6.65	6.17	92.71%
$x = 2$	6.63	5.43	81.91%

bulk $Yb_2W_3O_{12}$ and $Y_2W_3O_{12}$ reported [10]. The initial expansion and hygroscopy depend on the storage conditions of the samples. If the $Yb_{2-x}La_xW_3O_{12}$ ($x = 0$, 0.25, 0.5, 1, 1.5, 1.75) ceramics were stored in air, the samples will absorb moisture. It is reported that water molecules would occupy the crystallographic voids in hydrated $A_2W_3O_{12}$ structure, and the A–O–W linkages bend away from 180° due to the water molecules enter the compound. The incorporation of water in the framework structure will hinder the transverse vibrations of A–O–W linkages and prevent negative thermal expansion [9]. If the $Yb_{2-x}La_xW_3O_{12}$ ceramics were stored in a dry container, there is no initial expansion observed in the thermal expansion curves. As shown in Fig. 6(b), the $Yb_{1.75}La_{0.25}W_3O_{12}$ ceramics show negative thermal expansion in the entire testing temperature range.

For the other samples obtained in this experiment, the negative thermal expansion will occur after the complete removal of water, and this phenomena can be obviously observed in the thermal expansion curves of the $Yb_{2-x}La_xW_3O_{12}$ ($x = 0$, 0.5, 1, 1.5, 1.75) ceramics (see Fig. 6(a), (c), (d)–(f)). The $Yb_{2-x}La_xW_3O_{12}$ ($x = 0$, 0.5, 1, 1.5, 1.75) ceramics show negative thermal expansion above 140 °C, and Table 2 shows the average linear thermal expansion coefficients of the $Yb_{2-x}La_xW_3O_{12}$ ($x = 0$, 0.25, 0.5, 1, 1.5, 1.75, 2) in the corresponding temperature range. The average linear thermal expansion coefficients of the $Yb_{2-x}La_xW_3O_{12}$ ($x = 0$, 0.25, 0.5, 1, 1.5, 1.75) ceramics are calculated to be $-7.78 \times 10^{-6}\,K^{-1}$, $-5.02 \times 10^{-6}\,K^{-1}$, $-5.48 \times 10^{-6}\,K^{-1}$, $-3.81 \times 10^{-6}\,K^{-1}$, $-3.49 \times 10^{-6}\,K^{-1}$and $-3.21 \times 10^{-6}\,K^{-1}$, respectively.

Compared with the $Yb_{2-x}La_xW_3O_{12}$ ($x = 0$, 0.25, 0.5, 1, 1.5, 1.75) ceramics, there is no thermal expansion hysteresis

Table 2
Average linear thermal expansion coefficients of the $Yb_{2-x}La_xW_3O_{12}$ ($x = 0$, 0.5, 1, 1.5, 1.75, 2) ceramics.

$Yb_{2-x}La_xW_3O_{12}$	Temperature range (°C)	α_l ($\times 10^{-6}\,K^{-1}$)
$x = 0$	119–700	−7.78
$x = 0.25$	119–700	−5.02
$x = 0.5$	128–700	−5.48
$x = 1$	131–700	−3.81
$x = 1.5$	171–700	−3.49
$x = 1.75$	145–700	−3.21
$x = 2$	25–700	2.06

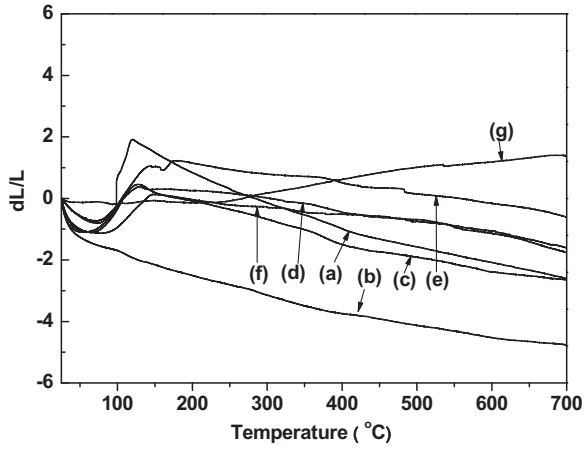

Fig. 6. Thermal expansion curves of the obtained $Yb_{2-x}La_xW_3O_{12}$ ($x = 0$, 0.25, 0.5, 1, 1.5, 1.75, 2) ceramics.

observed in the thermal expansion curve shown in Fig. 6(g). The non-hygroscopic monoclinic $La_2W_3O_{12}$ ceramic shows positive thermal expansion, and the average linear thermal expansion coefficient is calculated to be $2.06 \times 10^{-6}\,K^{-1}$ in the temperature range from 25 °C to 700 °C.

As seen from Table 2, it can be found that the average linear thermal expansion coefficients of the $Yb_{2-x}La_xW_3O_{12}$ ($x = 0$, 0.25, 0.5, 1, 1.5, 1.75, 2) become more negative with the increase of the content of ytterbium. We can interpret that the $Yb(La)O_6$ octahedra become larger with the increasing ytterbium content, and the oxygen–oxygen repulsion in polyhedra decrease. These factors make it easier for polyhedra to experience slight distortions, and the thermal expansion coefficient gets more negative. In this experiment, it can be obviously found that the thermal expansion coefficient of $Yb_{2-x}La_xW_3O_{12}$ ceramic can be easily controlled by adjusting the ration of ytterbium and lanthanum.

4. Conclusions

The new series of solid solutions $Yb_{2-x}La_xW_3O_{12}$ were prepared by solid state reaction. Pure phase of $Yb_{2-x}La_xW_3O_{12}$ can form in the composition range $0 \le x < 0.5$ with orthorhombic structure and $1.5 < x \le 2$ with monoclinic one. TG analysis shows that the $Yb_{2-x}La_xW_3O_{12}$ ($0 \le x \le 1.75$) is hygroscopic at room temperature and loses water in the temperature range from 40 °C to 80 °C. Compared with the $Yb_2W_3O_{12}$ and $La_2W_3O_{12}$, the densities of the samples $Yb_{2-x}La_xW_3O_{12}$ ($0.25 \le x \le 1.75$) were obviously improved. With the increase of the lanthanum content, the linear thermal expansion coefficients of the $Yb_{2-x}La_xW_3O_{12}$ decrease gradually. The thermal expansion properties of $Yb_{2-x}La_xW_3O_{12}$ can be adjust to be an anticipant value between $-7.78 \times 10^{-6}\,K^{-1}$ and $2.06 \times 10^{-6}\,K^{-1}$ by controlling the substitution ration of ytterbium and lanthanum.

Acknowledgments

The authors thank the Nation Natural Science Foundation of China (No. 51102207), Yangzhou Uinversity Development

Foundation for Talents (No. 0274640015427) and Yangzhou Uinversity Science and Technique Innovation Foundation (No. 2010CXJ081).

References

[1] J. Peng, M.M. Wu, H. Wang, Y.M. Hao, Z. Hu, Z.X. Yu, D.F. Chen, R. Kiyanagi, J.S. Fieramosca, S. Short, J. Jorgensen, Structures and negative thermal expansion properties of solid solutions $Y_xNd_{2-x}W_3O_{12}$ ($x = 0.0$–1.0, 1.6–2.0), J. Alloys Compd. 453 (2008) 49–54.

[2] P. Lommens, C.D. Meyer, E. Bruneel, K.D. Buysser, I.V. Driessche, S. Hoste, Synthesis and thermal expansion of ZrO_2/ZrW_2O_8 composites, J. Eur. Ceram. Soc. 25 (2005) 3605–3610.

[3] X.B. Yang, X.N. Cheng, X.H. Yan, J. Yang, T.B. Fu, J. Qiu, Synthesis of ZrO_2/ZrW_2O_8 composites with low thermal expansion, Compos. Sci. Technol. 67 (2007) 1167–1171.

[4] L.M. Sullivan, C.M. Lukehart, Zirconium tungstate (ZrW_2O_8)/polyimide nanocomposites exhibiting reduced coefficient of thermal expansion, Chem. Mater. 17 (2005) 2136–2141.

[5] Q.Q. Liu, J. Yang, X.N. Cheng, G.S. Liang, X.J. Sun, Preparation and characterization of negative thermal expansion $Sc_2W_3O_{12}$/Cu core–shell composite, Ceram. Int. 38 (2012) 541–545.

[6] J. Yang, Y.S. Yang, Q.Q. Liu, G.F. Xu, X.N. Cheng, Preparation of negative thermal expansion ZrW_2O_8 powders and its application in polyimide/ZrW_2O_8 composites, J. Mater. Sci. Technol. 26 (2010) 665–668.

[7] J.S.O. Evans, T.A. Mary, A.W. Sleight, Negative thermal expansion in $Sc_2(WO_4)_3$, J. Solid State Chem. 137 (1998) 148–160.

[8] J.S.O. Evans, T.A. Mary, A.W. Sleight, Negative thermal expansion in a large molybdate and tungstate family, J. Solid State Chem. 133 (1997) 580–583.

[9] S. Sumithra, A.M. Umarji, Hygroscopicity and bulk thermal expansion in $Y_2W_3O_{12}$, Mater. Res. Bull. 40 (2005) 167–176.

[10] S. Sumithra, A.M. Umarji, Role of crystal structure on the thermal expansion of $Ln_2W_3O_{12}$ (Ln = La, Nd, Dy, Y, Er and Yb), Solid State Sci. 6 (2004) 1313–1319.

[11] S. Sumithra, A.K. Tyagi, A.M. Umarji, Negative thermal expansion in $Er_2W_3O_{12}$ and $Yb_2W_3O_{12}$ by high temperature X-ray diffraction, Mater. Sci. Eng. B 116 (2005) 14–18.

[12] P.M. Forster, A. Yokochi, A.W. Sleight, Enhanced negative thermal expansion in $Lu_2W_3O_{12}$, J. Solid State Chem. 140 (1998) 57–158.

[13] P.M. Forster, A.W. Sleight, Negative thermal expansion in $Y_2W_3O_{12}$, Int. J. Inorg. Mater. 1 (1999) 123–127.

[14] M.M. Wu, J. Peng, Y.Z. Cheng, H. Wang, Z.X. Yu, D.F. Chen, Z.B. Hu, Structure and thermal expansion properties of solid solution $Nd_{2-x}Er_xW_3O_{12}$ ($0.0 \leq x \leq 0.6$ and $1.5 \leq x \leq 2.0$), Solid State Sci. 8 (2006) 665–670.

[15] X.L. Xiao, J. Peng, M.M. Wu, Y.Z. Cheng, D.F. Chen, Z.B. Hu, The crystal structure and thermal expansion properties of solid solutions $Ln_{2-x}Dy_xW_3O_{12}$ (Ln = Er and Y), J. Alloys Compd. 465 (2008) 556–561.

[16] M.M. Wu, J. Peng, Y.Z. Cheng, X.L. Xiao, Y.M. Hao, Z.B. Hu, Thermal expansion in solid solution $Er_{2-x}Sm_xW_3O_{12}$, Mater. Sci. Eng. B 137 (2007) 144–148.

[17] M.M. Wu, Y.Z. Cheng, J. Peng, X.L. Xiao, D.F. Chen, R. Kiyanagi, J.S. Fieramosca, S. Short, J. Jorgensen, Z.B. Hu, Synthesis of solid solution $Er_{2-x}Ce_xW_3O_{12}$ and studies of their thermal expansion behavior, Mater. Res. Bull. 42 (2007) 2090–2098.